B-spline modelling of inspiratory drive in NAVA-ventilated patients

Jennifer L. Knopp*, Ella Guy*, Kyeong Tae Kim*, Geoffrey M. Shaw, J. Geoffrey Chase***

**Department of Mechanical Engineering, University of Canterbury, Christchurch, New Zealand*

***Department of Intensive Care, Christchurch Hospital, Christchurch, New Zealand*

Corresponding author: Ella Guy (ella.guy@pg.canterbury.ac.nz)

Abstract: Model-based approaches are often used to estimate mechanical properties of lungs, such as elastance (E) and airway resistance (R), during invasive and non-invasive mechanical ventilation (MV). Current models are less effective when spontaneous breathing is present. This analysis utilises b-spline functions within a single compartment model framework to identify patient-specific inspiratory driving pressure. A series of 2nd-order, constrained b-spline basis functions are used to identify inspiratory driving pressure breath to breath alongside single E and R using inspiration and expiration data from n=20 breaths for 10 patients ventilated using NAVA. Median [IQR] per patient RMS error for n = 20 breaths was 0.75 [0.6 – 0.9] cmH_2O, with elastance ranging from 2.1 – 29.8 cmH_20/L, and per-patient median peak driving pressure ranging from -1.9 to -7.9 cmH_2O. Inspiratory driving pressure profiles matched esophageal pressures from literature and its value at peak nervous signal to the diaphragm (Eadi) was correlated with peak Eadi (R^2=0.25-0.86). Average trans-pulmonary pressure remained consistent between breaths for each patient, despite differences in peak Eadi and peak airway pressure. Overall, the model-based approach resulted in physiologically reasonable inspiratory driving pressures, with trends with electrical activity and matched literature data showing neuro-muscular decoupling as a function of pressure and/or volume.

Keywords: *Mechanical Ventilation; Spontaneous Breathing, NAVA, Single compartment model, B-spline*

1. INTRODUCTION

Model-based approaches are often used to estimate lung mechanics properties during mechanical ventilation (invasive or non-invasive) (Chiew et al., 2011, Chiew et al., 2013, Morton et al., 2019a) or out-patient spirometry (Howe et al., 2020a, Howe et al., 2020b). Lung elastance, or tissue stiffness, and airway resistance are commonly examined to assess lung function to optimise therapy (Chiew et al., 2011).

The single compartment model for lung mechanics is ubiquitous within the field as a simple and readily identifiable model for bedside identification of basic lung properties (Bates, 2009). The model has been validated in fully sedated patients (Chiew et al., 2011), where all or most of the work of breathing (WOB) is performed by the ventilator. Spontaneous breathing effort, though often clinically desirable (Gama de Abreu et al., 2012, Neumann et al., 2005, Wrigge et al., 2003), complicates model analyses and masks identification of respiratory parameters (Chiew et al., 2018, Major et al., 2016, Redmond et al., 2019).

In particular, the relative contribution of inspiratory effort, generating a negative driving pressure, and the opposing positive elastic pressure generated by volumetric expansion of the lung tissues, is difficult to elucidate from airway pressure alone. Measurements of inspiratory effort require an additional measurement, typically, esophageal pressure or the electrical activity of the diaphragm and/or surrounding musculature.

Spontaneous breathing effort is common, driving, normal tidal breathing, as well as tidal breathing in patients receiving CPAP ventilation or participating in spirometry for lung function analysis. It is very important in the lead up to patient weaning from (invasive and non-invasive) mechanical ventilation (Gama de Abreu et al., 2012), where sedation minimization is desired, and in neonatal ICU (Kim et al., 2018). Thus, models able to capture and separate spontaneous vs. passive breathing mechanics are important for future directions in model-based therapies and their patient-specific optimization.

This paper presents a simple, constrained b-spline model to estimate breath-to-breath spontaneous breathing effort in addition to lung elastance and airway resistance.

2. METHODS

2.1 Model

Basic lung physiology and mechanics are shown in Figure 1, modelled using spring and damping terms. If the pressure drop across the airways is considered proportional to flow, Q, the airway pressure (P_{aw}) is:

$$P_{aw} = P_a + RQ \tag{1}$$

Where P_a is alveolar pressure and R ($cmH_2O.s/L$) is airway resistance. Trans-pulmonary pressure, ΔP_{TP}, is characterized by lung elasticity (E_L, $cmH_2O.s/L$):

$$\Delta P_{TP} = P_a - P_p = E_L V \tag{2}$$

Where V is lung volume (L). A more correct model of Pleural pressure (P_p), includes gastric pressure (P_g), trans-diaphragmatic pressure (ΔP_{Di}), and chest wall recoil (E_{CW}):

$$P_p = \left(P_g + \Delta P_{Di}\right) + E_{CW} V \tag{3}$$

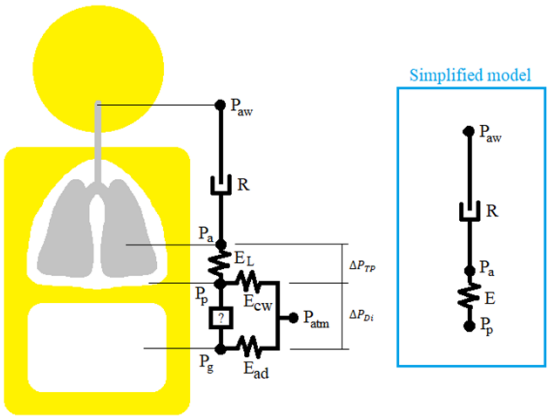

Figure 1: Spring-damper modelling of lung physiology.

However, Equation 3 can be simplified to:

$$P_a = EV + \hat{P_p} \tag{4}$$

Where $\hat{P_p}$ is inspiratory driving pressure resulting from gastric and trans-diaphragmatic pressures, and E (cmH₂O.s/L) includes elastic recoil from both the lung and chest wall. Thus, $\hat{P_p}$ is relative to a baseline pressure at end expiration at the set PEEP. Thus, Equation 1, with an applied PEEP, becomes:

$$P_{aw} = PEEP + EV + RQ + \hat{P_p} \tag{5}$$

Equation 5 is a modified version of the single compartment model (Bates, 2009), where V is tidal volume above end-expiratory volume at the current PEEP.

Inspiratory driving pressure, $\hat{P_p}$, is modelled using 2nd order (d=2) b-spline functions defined over time. First (d=0) and higher orders (d>0) are recursively defined [43, 44]:

$$\Phi_{i,0}(t) = f(x) = \begin{cases} 1, & T_i < t < T_i + 1 \\ 0, & otherwise \end{cases}$$

$$\Phi_{i,d}(t) = \frac{t - T_i}{T_{i+d} - T_i}\Phi_{i,d-1}(t) + \frac{T_{i+d+1} - t}{T_{i+d+1} - T_{i+1}}\Phi_{i+1,d-1}(t) \quad d \geq 1 \tag{6}$$

B-spline knots, T_i, are equally spaced division points in time. Splines are non-zero on $d + 1$ knot spans, and all splines sum 1.0 at any point in time. A knot width of 0.05 seconds is used here, so the number and range of b-splines varies with inspiration length. For each inspiration, $T_{max} = k_w \times \text{ceiling}(T_{insp}/k_w)$ defines the time span of all b-splines, and there are $M = T_{max}/k_w + d$ total b-splines.

Thus, $\hat{P_p}$ is the sum of M b-splines over inspiration (only):

$$\hat{P_p} = \sum_{i=1}^{M} -P_{s,i}\Phi_{i,2}(t) \tag{7}$$

Where $P_{s,i}$ are constant coefficients identified from measured data, and $\hat{P_p}$ is defined as a negative pressure generation. An example is shown in Figure 2. The overall modelled airway pressure is thus:

$$P_{aw} = PEEP + EV(t) + R(t)Q(t) - \sum_{i=1}^{M} P_{s,i}\Phi_{i,2}(t) \tag{8}$$

Linear least squares regression is performed using Matlab's (Mathworks, Natick, MA, USA) lsqlin function to identify lung properties (E, R) and breath-breath inspiratory driving pressure $(\hat{P_p})$ by identifying the $P_{s,i}$ terms from n breaths using a system of equations (Ax=b) with matrices defined:

$$A = \begin{bmatrix} V_1(t), & Q_1(t), & -\Phi_{1,1,2}(t), \dots -\Phi_{1,M,2}(t), & [0]_{(n-1)\times M} \\ \vdots & & & \vdots \\ V_n(t), & Q_n(t), & [0]_{(n-1)\times M}, & -\Phi_{n,1,2}(t), \dots -\Phi_{n,M,2}(t) \end{bmatrix}$$

$$b = \begin{bmatrix} P_{aw,1}(t) \\ \vdots \\ P_{aw,n}(t) \end{bmatrix} - PEEP \tag{9}$$

$$x = \left[E, R, P_{s,1,1} \dots P_{s,1,M}, \dots, P_{s,n,1}, \dots, P_{s,n,M}\right]^T$$

Where $P_{aw}(t)$ and $Q(t)$ are measured by the ventilator, and V(t) is integrated breath-by-breath from $Q(t)$. A single set of passive mechanical properties (E,R) is identified across $n = 20$ breaths. Using lsqlin, E and R and the first 75% of M b-spline function coefficients, $P_{s,i}$, for each breath are constrained positive. The remaining 25% of b-spline functions are not constrained enabling any presence of end-inspiratory patient effort against the ventilator to be captured.

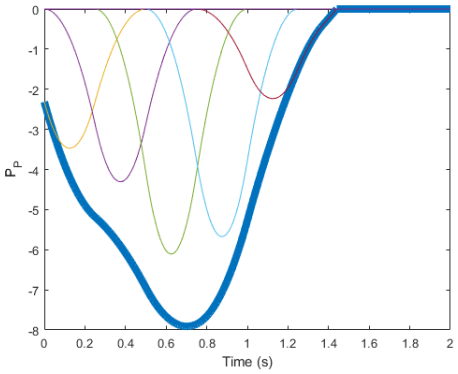

Figure 2: Example of inspiratory driving pressure constructed from 5 non-zero 2nd order b-spline functions.

The first 5 data points from expiration data were removed, as sudden pressure drop is deemed predominantly a function of ventilator and breathing circuit mechanics. Expiration data is also trimmed to data where expiratory $Q(t)$ is greater than 10% of peak expiratory flow. This ensures parameter identification is not heavily weighted towards expiration, which is approximately twice as long as inspiration.

2.2 Patients

This pilot analysis uses 10 patients ventilated on NAVA ventilation at the Cliniques Universitaires St-Luc (Brussels, Belgium) as part of a prospective crossover trial of PS and NAVA. Further details on the trial and inclusion/exclusion criteria can be found in (Piquilloud et al., 2011). Patients were ventilated on a Servo-I ventilator (Maquet, Solna, Sweden).

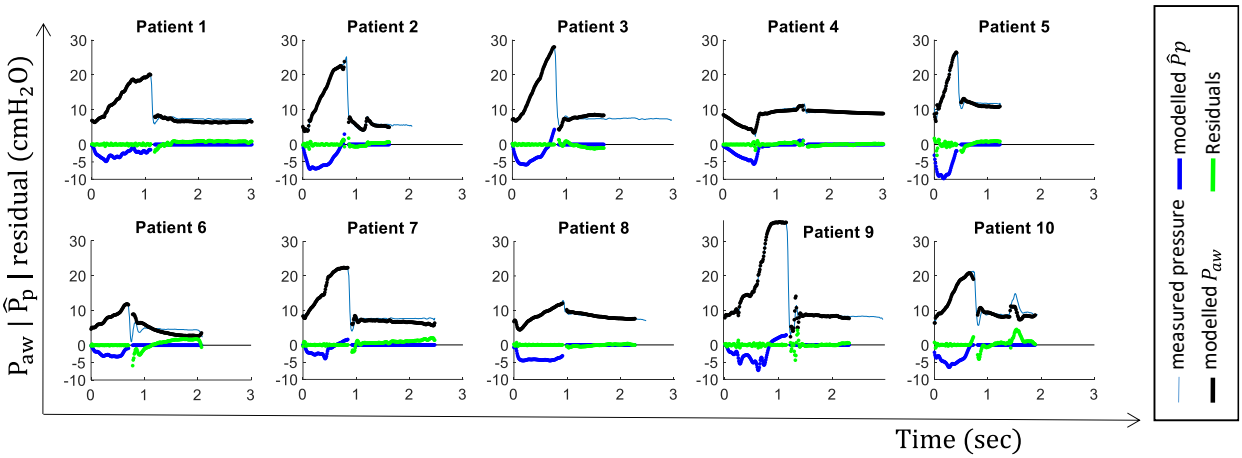

Figure 3: Examples of model-fit for a single breath from each patient. Lung mechanics are fit simultaneously over n = 20 breaths from each patient, but inspiratory drive ($\hat{P}_p$) is uniquely fit for each breath.

Following ventilation on PS, the ventilator was switched to NAVA, with the NAVA level set so the PIP was similar to that PS ventilation. Data was recorded for 20 minutes while on NAVA at 100 Hz. Ventilation outcomes are given in Table 1.

Inspiration and expiration were defined as positive and negative flow, respectively. Breaths with tidal volume less than 50mL, or where end expiratory volume was >50mL different from the expected 0mL, were discarded. End-inspiration was defined in two ways: ventilator-delivered inspiration ended when flow became negative, and patient-driven inspiration ended at peak Eadi. Typically, under NAVA, ventilator delivered end-inspiration occurs when Eadi has dropped to 70-80% of its peak value, and thus some patient-ventilator asynchrony may be present at this point.

2.3 Analyses

The model was identified over the first 20 breaths for each patient when on NAVA ventilation. Identification fit error is reported as median [IQR] per-patient RMS error. Correlation of PIP with peak Eadi assesses NAVA mode implimentation efficacy, while the correlation of tidal volume with PIP (V_t vs. PIP) reflects variability in delivered volume due to patient-specific and breath-specific variability in breathing effort on top of ventilator-delivered pressure. Linear regression is used, and y-intercepts are not constrained to go through (0,0). Mean $\hat{P}_p$ over patient-inspiration is plotted against mean $P_a = P_{aw} - RQ$, to assess whether outcomes fall along lines of constant trans-pulmonary pressure, as per the analysis of (Sinderby et al., 2007).

Table 1: NAVA ventilation outcomes for n = 20 breaths. Results are median [inter-quartile range] where relevant.

Pt	RR (1/min)	Vt (mL)	PEEP (cmH_2O)	T_{insp} (sec)	T_{exp} (sec)	PIP(cmH_2O)	Peak Eadi (μV)
1	12.8	0.6 [0.6 - 0.7]	7.2	1.21 [1.13 - 1.28]	3.39 [3.31 - 3.70]	22.4 [21.5 - 23.9]	635 [601 - 716]
2	31.9	0.4 [0.4 - 0.5]	5.4	0.74 [0.67 - 0.81]	1.18 [1.03 - 1.28]	21.2 [19.5 - 24.8]	417 [359 - 466]
3	20.1	0.4 [0.4 - 0.4]	7.3	0.73 [0.70 - 0.76]	2.19 [1.96 - 2.37]	23.8 [21.8 - 25.6]	1407 [1237 - 1561]
4	20.9	0.3 [0.3 - 0.3]	8.9	1.27 [1.16 - 1.38]	1.55 [1.45 - 1.63]	11.1 [10.5 - 11.7]	348 [304 - 392]
5	48.1	0.3 [0.3 - 0.3]	11.8	0.46 [0.43 - 0.50]	0.77 [0.73 - 0.83]	30.2 [27.2 - 33.5]	1947 [1617 - 2268]
6	29.5	0.5 [0.5 - 0.5]	4.4	0.72 [0.70 - 0.78]	1.28 [1.22 - 1.37]	16.0 [14.4 - 17.0]	2873 [2483 - 3117]
7	20.2	0.3 [0.3 - 0.4]	7.6	0.75 [0.71 - 0.82]	1.72 [1.54 - 2.42]	20.9 [18.4 - 24.5]	946 [780 - 1193]
8	24.2	0.3 [0.3 - 0.5]	7.5	0.92 [0.82 - 0.98]	1.64 [1.38 - 1.69]	13.6 [11.6 - 18.5]	442 [324 - 691]
9	20.6	0.5 [0.4 - 0.5]	8.2	1.06 [1.00 - 1.12]	1.86 [1.78 - 2.00]	32.2 [29.2 - 35.3]	290 [269 - 312]
10	30.7	0.4 [0.4 - 0.4]	8.6	0.71 [0.65 - 0.75]	1.21 [1.19 - 1.31]	21.6 [20.5 - 23.3]	2826 [2454 - 3182]

Table 2: Model-based outcomes over n = 20 breaths. Results are median [inter-quartile range] where relevant.

Pt	E (cmH_2O/L)	R ($cmH_2O/L/min$)	RMS (cmH_2O)	Airway driving pressure	Peak $\widehat{P_p}$(cmH20)	R^2 PIP vs. peak Eadi	R^2 V_t vs. PIP	R^2 $\widehat{P_p}$ vs. peak Eadi
1	11.5	10.8	0.8	15.2 [14.3 - 16.8]	-3.8 [-4.1 - -3.7]	0.97	0.84	0.85
2	25.4	7.2T	0.6	15.8 [14.1 - 19.3]	-5.3 [-5.7 - -5.1]	0.85	0.93	0.42
3	18.4	10.7	0.5	16.5 [14.5 - 18.3]	-4.5 [-4.7 - -4.3]	0.85	0.82	0.53
4	2.1	0.0	0.2	2.2 [1.6 - 2.8]	-3.2 [-4.6 - -2.7]	0.24	0.44	0.63
5	29.8	9.9	0.9	18.4 [15.4 - 21.7]	-7.9 [-8.8 - -7.3]	0.93	0.83	0.81
6	9.3	5.9	1.6	11.7 [10.0 - 12.6]	-1.9 [-2.4 - -1.4]	0.80	0.26	0.59
7	14.7	13.7	0.8	13.3 [10.8 - 16.9]	-2.2 [-2.9 - -1.9]	0.99	0.79	0.76
8	16.7	5.9	0.7	6.1 [4.1 - 11.0]	-3.8 [-4.2 - -3.4]	0.99	0.96	0.86
9	25.4	19.1	0.7	24.0 [21.0 - 27.1]	-7.3 [-8.2 - -6.0]	0.71	0.49	0.57
10	14.7	7.6	0.9	13.0 [11.9 - 14.6]	-4.0 [-4.4 - -3.7]	0.84	0.72	0.69

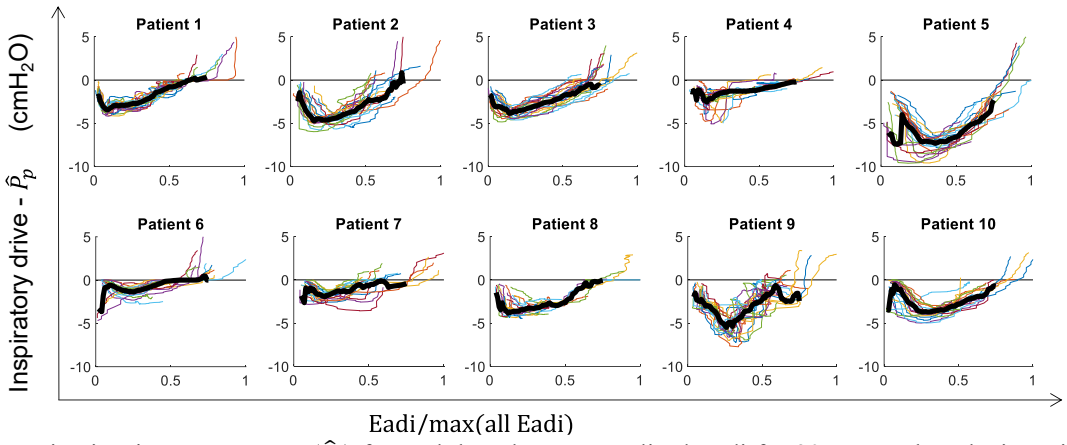

Figure 4: Negative inspiratory pressure ($\hat{P}_p$) for each breath vs. normalised Eadi for 20 NAVA breaths in a single model identification (n = 20) for each patient. Bold lines show the median inspiratory drive across Eadi.

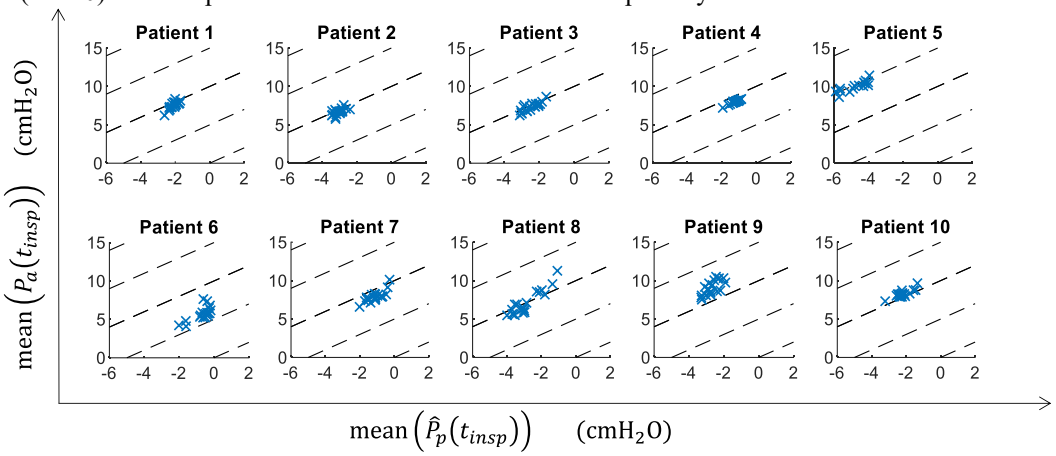

Figure 5: Inspiratory drive vs. alveolar pressure. Dashed lines represent constant trans-pulmonary pressure. Format adapted from (Sinderby et al., 2007)

3. RESULTS

Model-bsaed results are given in Table 2 and typical model fits are given in Figure 3. Median [IQR] per patient RMS error for n = 20 breaths was 0.75 [0.6 – 0.9] cmH_2O. RMS error over inspiration was lower at 0.25 [0.2 – 0.5] cmH_2O. Peak error typically occurred near peak expiratory flow, as shown in Figure 3, likely reflecting lung tissue relaxation time-constants currently not captured in the single compartment model (Bates, 2007, Ganzert et al., 2009, Schranz et al., 2011).

Correlation of PIP and peak Eadi is very high (R^2 = 0.71-0.99), as expected under NAVA (Verbrugghe and Jorens, 2011). Correlation of PIP with tidal volume resulted in regression constants varying from 0.26-0.93 with a median R^2 = 0.81.

Inspiratory effort in Figure 3 reflects expected shapes for net pleural pressure changes over inspiration, with peak negative pressure ranging from ~ -2 to -8 cmH20 (Table 2). Inspiratory drive is non-linear with Eadi, but generally consistent breath-breath within a patient. All patients in Figure 4 show positive inspiratory breathing effort at end of inspiration, suggesting mild patient-ventilator asynchrony during this period.

Correlation of pleural pressure ($\hat{P}_p$) with peak Eadi in Table 3 was moderately high, showing a reduction in the magnitude of breath-to-breath negative inspiratory driving with increasing Eadi. This end-inspiration reduction in negative inspiratory driving pressure with peak Eadi is likely due to ventilator unloading, where an increasing proportion of the work of breathing is done by the ventilator at higher support levels.

In Figure 5, average inspiratory effort vs. average alveolar pressure generally occurs along the dashed lines showing constant trans-pulmonary pressure. This result suggests patient WOB, and unloading of WOB onto the ventilator within a breath, is based on physiological feedback systems to maintain constant trans-pulmonary pressure, where the ventilator unloading onset is likely PEEP and NAVA level specific.

4. DISCUSSION

4.1 Model-based outcomes

A b-spline model was used to identify breath-breath inspiratory driving pressure alongside lung mechanics in patients on NAVA. Model results show physiologically reasonable inspiratory driving pressures, reflecting spontaneous breathing effort, with overall good model fit to data. The driving pressures are compared to the nervous electrical signal input to the diaphragm, Eadi, and correlations and trends show a measure of validation in model-identified inspiratory drive behavior.

The b-spline modelled inspiratory drive pressures match the shapes and variation magnitude within a breath for pleural or esophageal pressure in the literature (Imsand et al., 1994,

Lecomte et al., 2009, Mauri et al., 2016, Piquilloud et al., 2019, Sinderby et al., 2007), including peak negative esophageal pressure before PIP (Imsand et al., 1994, Mauri et al., 2016, Piquilloud et al., 2019, Sinderby et al., 2007) and incidence of positive pressure relative to baseline at breath end (Berger et al., 1996, Sinderby et al., 2007, Viale et al., 1998). The average trans-pulmonary pressure in Figure 6 is relatively constant across n =20 breaths, implying consistency in physiological feedback controlling breathing effort. Overall, the variability, shape and patterns of the inspiratory driving pressures identified are physiologically reasonable. Thus, the modelling approach may provide insight into patient breathing effort.

The modelling approach presented here captures relative pleural pressure changes over inspiration, as opposed to absolute pleural pressure. Physiologically, a baseline pleural end-expiration pressure offset is expected due to lung volume, lung tissue/chest wall properties, and diaphragm/abdominal pressures. Thus, these results are likely PEEP and NAVA level specific, but capture the variation in inspiratory driving pressure magnitude required to estimate WOB.

Consistency of trans-pulmonary pressure was analysed using the method of Sinderby et al, who showed consistency in trans-pulmonary pressure across NAVA levels in healthy subjects, despite a wider range of inspiratory driving pressure changes than analyzed here (Sinderby et al., 2007). The constant transpulmonary pressure seen differed between quiet breathing and stronger inspiratory efforts (Sinderby et al., 2007).

Inspiratory drive in Figure 4 was non-linear with Eadi, but consistent within a patient. Peak negative plural pressure did not occur with peak Eadi, suggesting non-linear conversion of electrical signals to diaphragm muscular action. Ventilator unloading, where the ventilator takes over the WOB as the breath progresses, is a known physiological phenomenon, which likely contributes to the non-linearity in the Eadi-pressure transformation shown. The results in Figures 3-4 also imply activation of physiological feedback control systems to avoid over distension and tissue damage.

In Table 2 and Figure 4, end inspiratory pleural pressure, $\widehat{\boldsymbol{P_p}}$, became more positive (lower inspiratory effort) at higher Eadi, with $R^2 = 0.42 – 0.86$. This result implies lower patient WOB as the NAVA level, and thus PIP, increases, matching trends in literature. This unloading of WOB on the ventilator, termed 'ventilator unloading,' occurs with increasing NAVA (Beck et al., 2003, Imsand et al., 1994, Lecomte et al., 2009, Sinderby et al., 2007) or pressure support (Amato et al., 1992, Berger et al., 1996, Brochard et al., 1987) level, as pressure and/or volume increases. Ventilator unloading results in a greater proportion of the WOB of breathing being done by the ventilator. Total unloading, where the ventilator delivers all or most of the work of breathing, is patient specific in its pressure setting (Berger et al., 1996), and is the standard critical care ventilation of sedated patients (Morton et al., 2019b).

In this analysis, lower inspiratory breathing efforts at higher Eadi, and the drop off in inspiratory driving pressure with Eadi in Figure 4, imply ventilator unloading occurs. Imsand et al show similar results within a breath, with a patient showing a drop in esophageal pressure early within a breath, followed by a pressure rise, which extends higher than baseline pressure at inspiration-onset near the end of the breath, at a trajectory parallel to that in passive breathing. They conclude active inspiration turned to passive inspiration within the same breath (Imsand et al., 1994).

4.2 Limitations

B-spline based models of spontaneous breathing effort are compared to measured Eadi and known behaviors as a first validation of the method. Further validation would require comparison to invasive esophageal pressures, which were not available in this study and are rarely measured.

This modelling approach may be less effective when airway pressure fluctuations are flatter, such as when high breathing effort is present or under CPAP ventilation. Patient 4 had relatively low variability in airway pressure, and the model elastance and resistance were low (2.1 cmH20/mL and 0 cmH20.s/mL), likely due to parameter trade-off between passive lung mechanics and negative driving pressure. However, overall model residuals are low, suggesting no missing dynamics. Flatter pressure profiles may necessitate further assumptions or regularization for identifiability, and the approach presented here is likely best in patients with stronger pressure profiles due higher ventilation requirements, which is also the cohort in which the model-based insights are potentially most useful.

The model is fit over a series of breaths to ensure passive lung properties (E, R) do not trade off with inspiratory breathing efforts. Model fit to multiple breaths, and including 'passive' expiration data, improves parameter identification of passive lung mechanics. The modelling approach also currently constrains inspiratory drive to be mostly negative over inspiration, regularizing the optimisation and identifiability problem (Docherty et al., 2011), and ensuring the optimal model fit is not a b-spline rendition of airway pressure with $E=0$ and $R=0$. Future work should explore constraint minimization and timing, as asynchrony commonly occurs around inspiration onset or early in a breath.

5. CONCLUSIONS

Second-order b-spline basis functions were used to identify inspiratory driving pressure breath to breath. Lung elastance ranging from 2.1 – 29.8 cmH_20/L, and per-patient median peak driving pressure ranging from -1.9 to -7.9 cmH_2O. Negative inspiratory driving pressure profiles matched esophageal pressures from literature, and showed trends with the electrical activity of the diaphragm. Average trans-pulmonary pressure remained consistent between breaths for each patient. Overall, the model-based method yielded physiologically reasonable inspiratory driving pressures, with trends with electrical activity. Results matched literature data showing neuro-muscular decoupling as a function of pressure and/or volume.

REFERENCES

Amato, M. B., Barbas, C. S., Bonassa, J., Saldiva, P. H., Zin, W. A. & de Carvalho, C. R. 1992. Volume-assured pressure support ventilation (VAPSV). A new approach for reducing muscle workload during acute respiratory failure. *Chest,* 102**,** 1225-34.

Bates, J. 2007. A Recruitment Model of Quasi-Linear Power-Law Stress Adaptation in Lung Tissue. *Annals of Biomedical Engineering,* 35**,** 1165-1174.

Bates, J. H. T. 2009. The linear single-compartment model. *In:* BATES, J. H. T. (ed.) *Lung Mechanics: An Inverse Modeling Approach.* Cambridge: Cambridge University Press.

Beck, J., Spahija, J. & Sinderby, C. Respiratory Muscle Unloading during Mechanical Ventilation. 2003 New York, NY. Springer New York, 280-287.

Berger, K. I., Sorkin, I. B., Norman, R. G., Rapoport, D. M. & Goldring, R. M. 1996. Mechanism of relief of tachypnea during pressure support ventilation. *Chest,* 109**,** 1320-7.

Brochard, L., Pluskwa, F. & Lemaire, F. 1987. Improved efficacy of spontaneous breathing with inspiratory pressure support. *Am Rev Respir Dis,* 136**,** 411-5.

Chiew, Y. S., Chase, J. G., Shaw, G., Sundaresan, A. & Desaive, T. 2011. Model-based PEEP optimisation in mechanical ventilation. *BioMed Eng OnLine,* 10.

Chiew, Y. S., Chase, J. G., Lambermont, B., Roeseler, J., Pretty, C., Bialais, E., Sottiaux, T. & Desaive, T. 2013. Effects of Neurally Adjusted Ventilatory Assist (NAVA) levels in non-invasive ventilated patients: titrating NAVA levels with electric diaphragmatic activity and tidal volume matching. *Biomed Eng Online,* 12**,** 61.

Chiew, Y. S., Tan, C. P., Chase, J. G., Chiew, Y. W., Desaive, T., Ralib, A. M. & Mat Nor, M. B. 2018. Assessing mechanical ventilation asynchrony through iterative airway pressure reconstruction. *Comput Methods Programs Biomed,* 157**,** 217-224.

Docherty, P. D., Chase, J. G., Lotz, T. F. & Desaive, T. 2011. A graphical method for practical and informative identifiability analyses of physiological models: a case study of insulin kinetics and sensitivity. *Biomed Eng Online,* 10**,** 39.

Gama de Abreu, M., Guldner, A. & Pelosi, P. 2012. Spontaneous breathing activity in acute lung injury and acute respiratory distress syndrome. *Curr Opin Anaesthesiol,* 25**,** 148-55.

Ganzert, S., Möller, K., Steinmann, D., Schumann, S. & Guttmann, J. 2009. Pressure-dependent stress relaxation in acute respiratory distress syndrome and healthy lungs: an investigation based on a viscoelastic model. *Crit Care.,* 13**,** R199.

Howe, S. L., Marz, M., Kruger-Ziolek, S., Laufer, B., Pretty, C., Shaw, G. M., Desaive, T., Moller, K. & Chase, J. G. 2020a. Measuring lung mechanics of expiratory tidal breathing with non-invasive breath occlusion. *Biomed Eng Online,* 19**,** 32.

Howe, S. L., Marz, M., Pinter, J., Kruger-Ziolek, S., Pretty, C., Shaw, G. M., Desaive, T., Moller, K. & Chase, J. G. 2020b. Cheek support affects lung mechanics measurements of tidal-based spontaneous breathing. *Comput Methods Programs Biomed,* 193**,** 105526.

Imsand, C., Feihl, F., Perret, C. & Fitting, J. W. 1994. Regulation of Inspiratory Neuromuscular Output during Synchronized Intermittent Mechanical Ventilation. *Anesthesiology,* 80**,** 13-22.

Kim, K. T., Howe, S., Chiew, Y. S., Knopp, J. & Chase, J. G. 2018. Lung Mechanics in Premature infants: Modelling and clinical validation. *IFAC-PapersOnLine,* 51**,** 225-230.

Lecomte, F., Brander, L., Jalde, F., Beck, J., Qui, H., Elie, C., Slutsky, A. S., Brunet, F. & Sinderby, C. 2009. Physiological response to increasing levels of neurally adjusted ventilatory assist (NAVA). *Respir Physiol Neurobiol,* 166**,** 117-24.

Major, V., Corbett, S., Redmond, D., Beatson, A., Glassenbury, D., Chiew, Y. S., Pretty, C., Desaive, T., Szlávecz, Á., Benyó, B., Shaw, G. M. & Chase, J. G. 2016. Respiratory mechanics assessment for reverse-triggered breathing cycles using pressure reconstruction. *Biomedical Signal Processing and Control,* 23**,** 1-9.

Mauri, T., Yoshida, T., Bellani, G., Goligher, E. C., Carteaux, G., Rittayamai, N., Mojoli, F., Chiumello, D., Piquilloud, L., Grasso, S., Jubran, A., Laghi, F., Magder, S., Pesenti, A., Loring, S., Gattinoni, L., Talmor, D., Blanch, L., Amato, M., Chen, L., Brochard, L., Mancebo, J. & Group, P. L. p. w. 2016. Esophageal and transpulmonary pressure in the clinical setting: meaning, usefulness and perspectives. *Intensive Care Med,* 42**,** 1360-73.

Morton, S. E., Knopp, J. L., Chase, J. G., Moller, K., Docherty, P., Shaw, G. M. & Tawhai, M. 2019a. Predictive Virtual Patient Modelling of Mechanical Ventilation: Impact of Recruitment Function. *Ann Biomed Eng,* 47**,** 1626-1641.

Morton, S. E., Knopp, J. L., Chase, J. G., Docherty, P., Howe, S. L., Möller, K., Shaw, G. M. & Tawhai, M. 2019b. Optimising mechanical ventilation through model-based methods and automation. *Annual Reviews in Control*.

Neumann, P., Wrigge, H., Zinserling, J., Hinz, J., Maripuu, E., Andersson, L. G., Putensen, C. & Hedenstierna, G. 2005. Spontaneous breathing affects the spatial ventilation and perfusion distribution during mechanical ventilatory support. *Crit Care Med,* 33**,** 1090-5.

Piquilloud, L., Vignaux, L., Bialais, E., Roeseler, J., Sottiaux, T., Laterre, P. F., Jolliet, P. & Tassaux, D. 2011. Neurally adjusted ventilatory assist improves patient-ventilator interaction. *Intensive Care Med,* 37**,** 263-71.

Piquilloud, L., Beloncle, F., Richard, J.-C. M., Mancebo, J., Mercat, A. & Brochard, L. 2019. Information conveyed by electrical diaphragmatic activity during unstressed, stressed and assisted spontaneous breathing: a physiological study. *Annals of Intensive Care,* 9**,** 89.

Redmond, D. P., Chiew, Y. S., Major, V. & Chase, J. G. 2019. Evaluation of model-based methods in estimating respiratory mechanics in the presence of variable patient effort. *Computer Methods and Programs in Biomedicine,* 171**,** 67-79.

Schranz, C., Knöbel, C., Kretschmer, J., Zhao, Z. & Möller, K. 2011. Hierarchical parameter identification in models of respiratory mechanics. *IEEE transactions on biomedical engineering,* 58**,** 3234-3241.

Sinderby, C., Beck, J., Spahija, J., de Marchie, M., Lacroix, J., Navalesi, P. & Slutsky, A. S. 2007. Inspiratory muscle unloading by neurally adjusted ventilatory assist during maximal inspiratory efforts in healthy subjects. *Chest,* 131**,** 711-717.

Verbrugghe, W. & Jorens, P. G. 2011. Neurally adjusted ventilatory assist: a ventilation tool or a ventilation toy? *Respir Care,* 56**,** 327-35.

Viale, J. P., Duperret, S., Mahul, P., Delafosse, B., Delpuech, C., Weismann, D. & Annat, G. 1998. Time course evolution of ventilatory responses to inspiratory unloading in patients. *Am J Respir Crit Care Med,* 157**,** 428-34.

Wrigge, H., Zinserling, J., Neumann, P., Defosse, J., Magnusson, A., Putensen, C. & Hedenstierna, G. 2003. Spontaneous breathing improves lung aeration in oleic acid-induced lung injury. *Anesthesiology,* 99**,** 376-84.